Article

A Reflective Spectroscopy and Mineralogical Investigation of Cosmetic Blush (Wet'N'Wild) Potentially for Forensic Investigations Related to Interpersonal Violence—An Experimental Feasibility Study

Juliana Curtis [1], Landon Stitle [1], Jessica Certain [1], Madeline Murchland [1], Charlotte Piszel [1], Jordan Vest [1], Claire L. McLeod [1] and Mark P. S. Krekeler [1,2,*]

1   Department of Geology and Environmental Earth Science, Miami University, Shideler Hall, Oxford, OH 45056, USA; curtisjc@miamioh.edu (J.C.); stitlele@miamioh.edu (L.S.); piszelcl@miamioh.edu (C.P.)
2   Department of Mathematical and Physical Sciences, Miami University Hamilton, Hamilton, OH 45011, USA
*   Correspondence: krekelmp@miamioh.edu

Abstract: Interpersonal violence is a rising issue in global society and new approaches are being sought to combat the problem. Within this context, expanding forensic techniques to better document violent crime scenes is critical for improving and acquiring legal evidence, such as proving or tracing contact between victims and suspects. This project aims to demonstrate the potential for forensic investigations in the context of interpersonal violence using a field-based reflective spectroscopy approach. For this, a common cosmetic, Wet'N'Wild "Color Icon" blush in the shade "Pearlescent Pink", was mineralogically characterized using transmission electron microscopy and powder X-ray diffraction and subsequently investigated via reflective spectroscopy on a variety of common substrates. Differing amounts of the cosmetic product, ranging from 0.001 g to 0.075 g, were applied to a variety of substrates using a simple push method to simulate forcible contact and material transfer. Substrates included a pine wood block; (calcareous) sand from Tulum, Mexico; Ottawa sand; tile; Pergo wood; linoleum; closet material; carpets; and fabrics. The reflective spectra of cosmetic–substrate combinations were measured via an ASD FieldSpec 4 Hi-Res spectroradiometer. The Wet'N'Wild cosmetic was reliably detected on various substrates relevant to crime scenes. Minor amounts (as low as $0.02 \ mg/mm^2$) could be detected, and average limits of detection of $0.03 \ mg/mm^2$ were achieved; however, a calcareous sand (Tulum) had a high level of detection ($>0.38 \ mg/mm^2$), suggesting that further investigation is needed for more complex sand substrates. The use of the ASD spectroradiometer as a forensic tool within the context of crime scene documentation shows promise. Future work should expand the characterization of cosmetic materials across a broad range of substrates and consider systematic studies of specific population groups. Furthermore, combining this approach with hyperspectral imaging at crime scenes is a promising future direction for crime scene documentation. This work therefore demonstrates a novel method for investigating cosmetics within the context of interpersonal violence and provides a foundation for future laboratory and field work using the ASD FieldSpec 4 and hyperspectral imaging systems.

Keywords: reflective spectroscopy; cosmetics; talc; violence

1. Introduction

Makeup is a term used to describe a variety of cosmetic products which are variably applied to human skin. These products are predominantly composed of clay minerals; commonly talc and kaolin, inorganic color additives, and glitter or shimmer particles [1–4]. As a fine-grained material that is present on the surface of skin, makeup has a high potential to be easily transferred via direct contact either from skin to skin or from skin to other

surfaces. Within the context of interpersonal violence, makeup can be transferred to numerous materials that may be present as substrates throughout crime scenes, such as tile, carpet, or wood. The detection of makeup therefore has the potential to contribute more evidence to forensic investigations and support crime scene characterization. It is noted here that we use the term "interpersonal violence" in line with the following definition: "Interpersonal violence involves the intentional use of physical force or power against other persons by an individual or small group of individuals. This can be further divided into family or partner violence, and community violence" [5].

Investigating cosmetics in the context of forensics has been done for at least the past 100 years. For example, in 1912 French forensic scientist Edmund Locard linked the composition of scrapings found underneath a potential perpetrator's fingernail to the composition of cosmetic powder on the victim's neck. In this case, the perpetrator was convicted of premeditated murder [6,7]. While the ability of cosmetic products to be utilized as forensic evidence was documented over a century ago, this approach was not significantly exploited until the 1980s [7]. Historically, the investigation of cosmetic materials within these contexts has taken place via liquid chromatography, molecular spectroscopy, atomic spectroscopy, and gas chromatography-mass spectrometry. Collectively, as of 2019, these techniques account for 86% of the analytical techniques used within the context described above [7]. More recent efforts have reported the successful use of portable energy dispersive X-ray fluorescence (EDXRF), attenuated total reflectance-Fourier transform infrared spectroscopy (ATR-FTIR) and Raman spectroscopy with a growing need for field-transportable, inexpensive, and non-destructive techniques [7–17]. With respect to the nature of the cosmetic product being characterized, lipsticks, nail polishes, and eye make-up have received the most attention [7,9–17].

With makeup products often being applied to the face and with that area commonly sustaining injury during a domestic violence case, using makeup transfer (smudges [10]) as evidence at the scene of the incident has the potential to significantly contribute to crime scene documentation. In addition to direct injury to the head, face, and neck area in domestic violence acts, one additional area of investigation that may be enhanced by a better understanding of makeup in crime scenes is sexual violence crimes, as transfer of cosmetics has the potential to occur in these scenarios also. Developing physical evidence-based tools for the investigation of sexual violence crimes would therefore be of benefit, particularly as sexual violence crimes tend to be underreported due to various fears the victim may face and various obstacles that come with reporting this type of crime [9,18,19].

The goal of this study is to therefore evaluate the feasibility of reflective spectroscopy, specifically using an ASD spectroradiometer, as a field-portable and rapid forensic tool. As an analog for multiple forms of mineral-based cosmetics, a common blush product was selected for this feasibility study. If sample materials can be detected on multiple and diverse substrates, then reflective spectroscopy shows promise as a field-based forensic investigative tool.

2. Materials and Methods

2.1. Materials

For this work, samples of the common makeup brand Wet'N'Wild were purchased. The Wet'N'Wild brand was chosen for this study due to its affordability and common occurrence at a wide range of retailers. All of the makeup products investigated were in powder form and included blush of the same shade and type. Specifically, four samples of Wet'N'Wild blush in the shade "Pearlescent Pink" from the "Color Icon Blush" line were purchased and investigated (Figure 1). Blush was chosen as the target makeup product due to its high surface area on one's face, therefore being more likely to be transferred onto a substrate. The ingredient list for the cosmetic product was also cataloged and is provided in Supplementary Table S1.
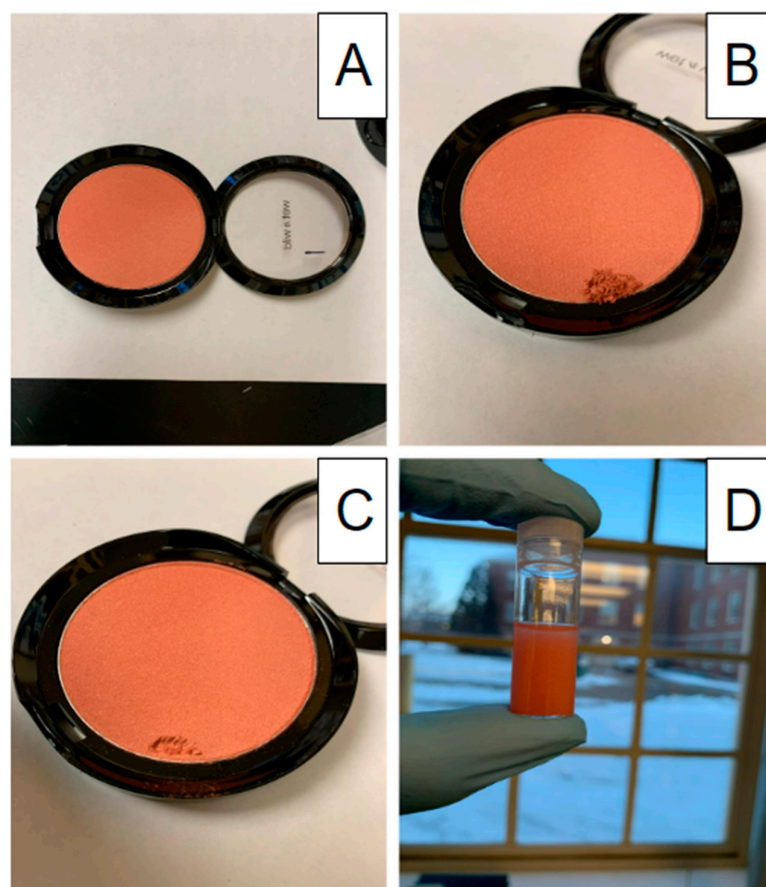
Figure 1. Example images of Wet'N'Wild blush showing an unmodified sample in (**A**) and samples with divets taken for analytical work in (**B**,**C**). Panel (**D**) shows a vial of a sample in suspension to be used for TEM analysis.

Sample–substrate combinations for this study were designed to simulate the transfer by forceful impact of a blush-covered surface (human skin) with another substrate, which generates a "smudge" [10]. By this means, the analogous abundance and application patterns of makeup that could be detected because of a violent crime were documented and characterized. Makeup materials were transferred to the substrates through a forceful shove with a nitrile gloved finger with the specific makeup mass placed on the substrate within the confines of a round plastic stencil area (196.07 mm^2). The stencil was used for repeatability and consistency in the area available for the ASD spectroradiometer to measure reflective light spectra.

The substrates onto which makeup was transferred in this study included flooring materials (carpet, linoleum, and Pergo wood), common clothing fabric (Khaki, denim, and white cotton), bathroom and closet materials (tile and closet components), and common outdoor materials (pine wood blocks, quartz-rich Ottawa sand, and Tulum carbonate sand). These substrates represent a wide range of materials and were selected based on their likely occurrence in potential crime scenes.

2.2. Methods

2.2.1. Powder X-ray Diffraction (XRD)

Basic powder X-ray diffraction analysis was used to identify major mineral phases in the Wet'N'Wild blush with a Bruker D8 Advance X-ray diffractometer (Bruker, Billerica, MA, USA) using Cu Kα radiation. Five aliquots of powder from a single Wet'N'Wild blush product were analyzed three times as rotating pack mounts from 2° to 75° 2θ, with a step size of 0.05° 2θ at 7.5 s/step.

2.2.2. Transmission Electron Microscopy (TEM) Methods

Four aliquots of Wet'N'Wild blush were loosened using a small clean metal probe and transferred to weigh paper. Sample masses ranged from 0.01 to 0.03 g, 0.02 g, 0.01 g, 0.03 g, and 0.02 g, respectively.

Each of the four aliquots were placed in ethanol-cleaned glass vials to which approximately 2 mL of ethanol was added. Each vial was then agitated by hand for 3 min and allowed to settle for 10 min. Lacey Formvar Carbon-Cu grids (300 mesh, 50 μm openings) (lot 181102) from Electron Microscopy Services were placed on clean glass slides. An ~2 μL volume of each sample suspension was deposited on each respective grid.

For bright-field TEM analysis, the samples were analyzed using a JEOL JEM 2100 TEM (Jeol Ltd., Akishima, Tokyo, Japan) operated at 200 kV at the Center for Advanced Microscopy and Imaging (CAMI) at Miami University. The instrument is equipped with a Bruker Quantax 200 STEM EDXS system. The TEM methods detailed above have been used in several previous investigations [20–26].

EDS analysis of fine-grained mixed mineral or mixed-phase samples with multiple chemical components requires an understanding of peak overlap and the limitations of signal contributions from multiple minerals, phases, and substrates. The lines used to identify elements were provided by Bruker software. The ubiquitous nature of oxygen, the scatter from the copper grid, and the lacey carbon substrates that contribute to EDS spot spectra are reported and discussed.

For talc, regarding crystallographic notation with respect to the use of Miller indices, by convention, the triclinic systematic would require the longest axis to be defined as the c-axis. Some researchers follow this convention and thus designate the staking direction as being along (0k0) [27]. For the convention specifically followed in the clay mineral and phyllosilicate literature, the stacking of 2:1 layers is in the (00l) direction and the b-axis or (0k0) functionally contains the most crystallographic complexity, as details of the stacking direction are most evident [28]. We elected to use notation in the tradition of Bailey for all phyllosilicates [28].

2.2.3. Spectroradiometry

For reflective spectra measurements, an ASD (PANalytical) FieldSpec 4 Hi-Res spectroradiometer (Malvern Panalytical, Malvern, UK) was utilized, which is a field portable instrument that can be used in a wide range of settings (including crime scenes) due to its versatility in both indoor and outdoor environments. The ASD FieldSpec 4 Hi-Res spectroradiometer has a spectral range of 350 to 2500 nm, with spectral resolutions of 3 nm at 700 nm and 8 nm at 1400 nm and 2100 nm. The instrument is equipped with a post-dispersive system for extremely low-stray light, which is at <0.02% for 350 to 1000 nm and <0.1% for 1000 to 2500 nm. The instrument uses a modular silicon array, as well as a Peltier cooled InGaAs detector spectrometer platform. The values for low noise equivalent delta radiance (NeDL) are 1.1×10^{-9} W/cm^2/sr/nm at 700 nm for UV/VNIR, 2.8×10^{-9} W/cm^2/sr/nm at 1400 nm for NIR, and 5.6×10^{-8} W/cm^2/sr/nm at 2100 nm. Several previous versions of the ASD (PANalytical) FieldSpec 4 Hi-Res have been produced, and prior work has utilized this technology in a range of settings and contexts [20,29–33].

Spectral features and bond assignments for the studied Wet'N'Wild cosmetic blush are provided in each respective spectral figure. The reflective spectroscopy literature and the USGS spectral library were used to determine bond assignments [34–41]. Assignments were in part informed by knowledge of the ingredients list supplied by the manufacturer (Supplementary Table S1). Studied sample aliquots contained both mineralogical and organic molecule features. Within the spectra that were measured, common features showed OH and water adsorption features (e.g., 1392 nm and 1413 nm (OH in minerals)), talc and phyllosilicates (e.g., 2310 nm (Mg-OH in talc)), and 2200 nm (Al-OH in muscovite)), reflective highs associated with Fe-bearing minerals (e.g., 535 nm and 700 nm), and adsorption features corresponding to possibly numerous organic molecules (e.g., 1730 nm (c-H) and 1690 nm (C-OH)). Additional specific spectral feature assignments and identifications for

substrate materials were made using data from the USGS spectral library as well as several long-standing reflective spectra references [34–41].

Data acquisition methods for this study were adapted for this investigation from recent papers and are very similar [31,32,42,43]. Flat plastic Petri dishes were painted black and used as an experimental substrate for reflective spectra measurements. For reference spectra, four replicate end member examples of blush measuring approximately 1 g were placed as a powder 1–2 mm thick in the center of each Petri dish to fill the field of view. Reflective spectroscopy measurements were acquired under open path illumination using the ASD (PANalytical) FieldSpec 4 Hi-Res spectroradiometer with a fiber-to-sample distance of approximately 50 cm. The spectra for each sample were collected at 1 s intervals, and 5 spectra were averaged for each spectrum measurement using the RS^3 software.

3. Results and Interpretations

### 3.1. Powder X-ray Diffraction (XRD)

The powder XRD scans indicated that the major mineral phases in the Wet'N'Wild cosmetic blush are muscovite and talc (Figure 2). Additional phases that were identified included rutile, quartz, goethite, chlorite, and lazurite (Figure 2). The powder XRD data showed minimal variation of the major phases present. However, there appears to be a significant discrepancy between the XRD data collected and the ingredient list reported for the product (Figure 2). For example, mica (or muscovite), which is characterized by an ~10 Å (001) peak, is not specifically listed but is possible (see Supplementary Table S1). Chlorite was observed, as indicated by the presence of an ~14 Å (001) peak and a weak potential (002) peak, which may have potential contributions from serpentine minerals (Figure 2).
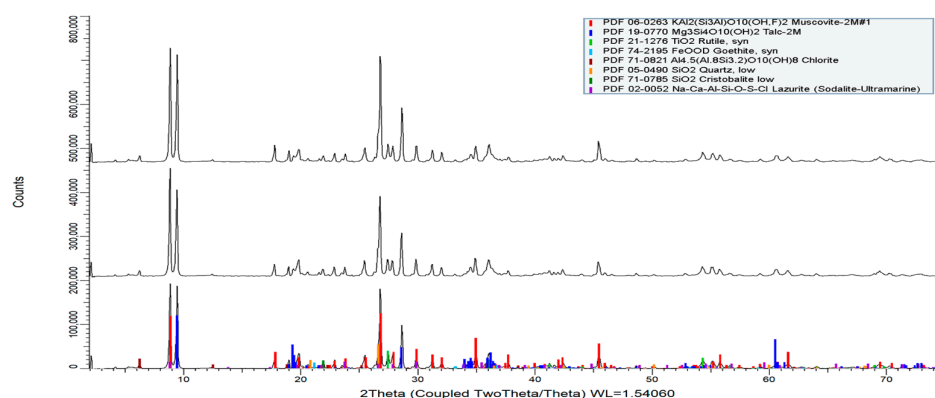
Figure 2. Representative basic powder XRD patterns of Wet'N'Wild blush with the major phases identified and PDF cards. Note that there are low-angle peaks that may be smectite minerals or organo-smectite intercalates. Additionally, the (002) peak of chlorite may potentially have contributions from serpentine, which cannot be resolved using basic powder X-ray diffraction (see text for discussion).

3.2. Transmission Electron Microscopy (TEM)

Representative bright-field TEM data are presented in Figure 3 and show common examples of size, morphology, electron diffraction, and EDS spectra for each dominant phyllosilicate. Muscovite generally shows sharp reflections, while talc generally shows some degree of pronounced stacking disorder (Figure 3). Although muscovite and talc morphologies are similar, they can easily be discerned by their EDS spectra. Based on the abundance and nature of these minerals, they are expected to strongly influence the nature of reflective spectra. Minor rutile, goethite, and chlorite were also observed in TEM data (not shown); however, lazurite was not. The data acquired via TEM are thus broadly consistent with the XRD data.
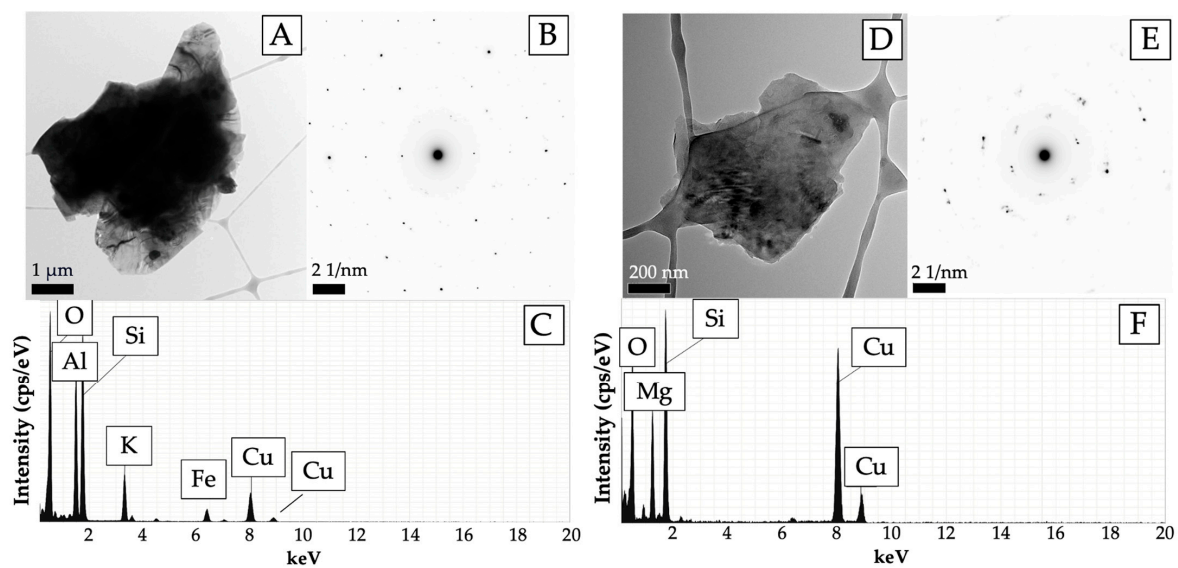
Figure 3. Panels (**A**–**C**) summarize a dataset for representative platy muscovite particles, with (**A**) being a bright-field image with a scale bar of 1 μm, (**B**) an electron diffraction pattern of ~(hk0) showing sharp reflections, and (**C**) an EDS spectrum with abundant Al, Si, and K, consistent with the presence of muscovite. Panels (**D**–**F**) summarize a dataset for representative platy talc particles, with (**D**) being a bright-field image with a scale bar of 200 nm, (**E**) an electron diffraction pattern of ~(hk0) [28] (or (h0l) [27]) showing stacking disorder, and (**F**) an EDS spectrum with abundant Mg and Si, consistent with talc. The Cu peak is attributed to the grid.

Although the Wet'N'Wild cosmetic blush was not specifically investigated for asbestos, talc fibers were observed. Figure 4 shows representative images of talc fibers (>3:1 aspect ratio), an electron diffraction pattern of ~(hk0) (or [h0l] [27]) showing stacking disorder, and EDS spectra with Mg and Si being abundant. Collectively, these observations are consistent with talc. It is noted here that talc fibers were much less abundant than talc or mica particles and were estimated to be <0.5% of the population of particles.
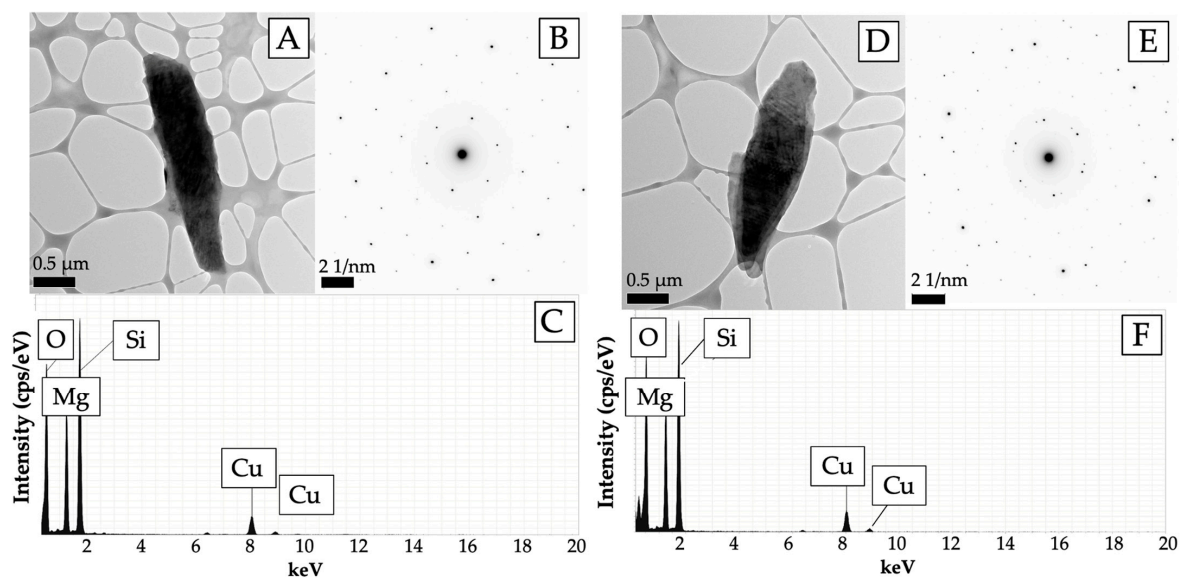

Figure 4. Representative images of talc fiber particles (>3:1 aspect ratio), with the panels in (**A**,**D**) being bright-field images with scale bars of 0.5 μm, (**B**,**E**) electron diffraction patterns of ~(hk0) [28] (or (h0l) [27]) showing stacking disorder, and (**C**,**F**) an EDS spectrum with abundant Mg and Si being abundant, consistent with talc. The Cu peak is attributed to the grid.

3.3. Reflective Spectroscopy

Reference reflective spectra for the Wet'N'Wild blush, collected in a black Petri dish, are provided in Figure 5, with major features identified. Figures 6–9 present reflective spectra from varying masses of blush on the variety of substrates investigated. Figure 6 shows spectra for makeup-bearing indoor flooring materials, including light and dark carpet samples, a medium-toned linoleum, and Pergo synthetic wooden flooring. Figure 7 shows spectra for makeup-bearing clothing fabrics, including khaki, denim, and white cotton. Figure 8 shows spectra relating to materials associated with, or expected in, bathrooms, including white tile, light brown tile, and a khaki fabric with cardboard (hanging organizer). The spectra shown in Figure 9 are associated with materials that may be found outdoors, with Ottawa sand representing common quartz rich sand, carbonate sands from Tulum Mexico representing calcareous environments, and a common pine 2″ × 4″ board.
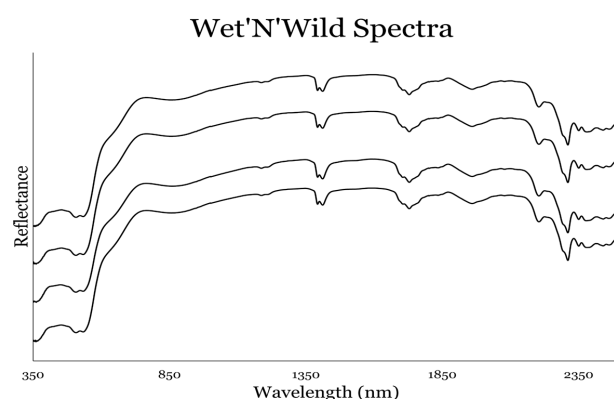

Figure 5. Four replicate spectra for Wet'N'Wild blush. The major features are interpreted to be as follows: ~350 nm (Mn and Fe), weak doublet at 506 nm (S) and 535 nm (Fe^{3+}), weak doublet at 1185 nm 1205 nm (OH and C-H), 1392 nm and 1413 nm (OH in minerals), triplet centered on 1730 nm (C-H), 1960 nm (C-OH), (G) 2200 nm (Al-OH, C-H, C-O, C=O, and N-H), and (H) 2310 nm (Mg-OH, Al-OH, and OH).
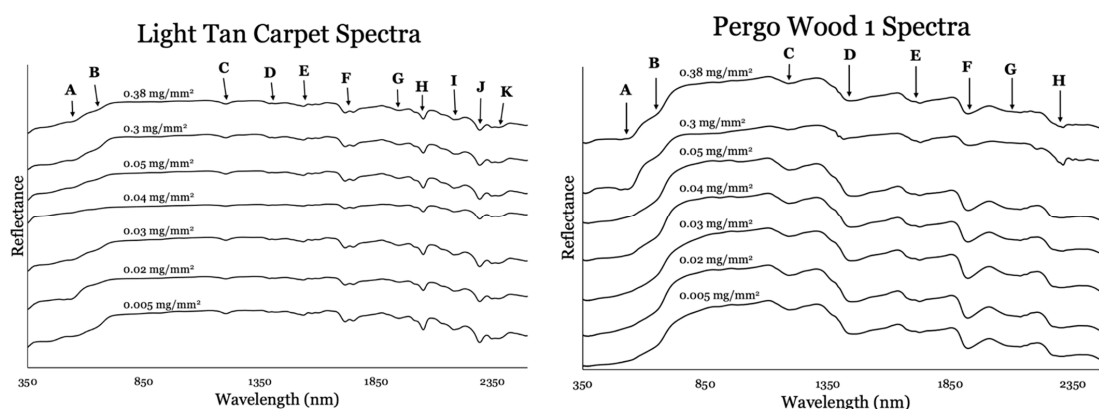
Figure 6. Spectra for floor materials. Carpet 1: Spectra for blush on light tan carpet, with major features and interpreted causes being (A) weak inflection at ~535 nm (Fe^{3+}), (B) weak inflection at 700 nm (Fe^{3+}), (C) 1205 nm (OH and C-H), (D) 1385 nm (H_2O), (E) 1583 nm (C-OH), (F) doublet at 1704 and 1760 nm (C-H), (G) 1875 nm (H_2O/OH), (H) 1940 nm (top) grading into 2040 nm (change in OH type), (I) 2182 nm (C-H, C-O, C=O, and N-H), (J) 2310 nm (Mg-OH, Al-OH, and OH), and (K) weak doublet at 2346 and 2376 (C-H). Pergo Wood 1: Spectra for blush on Pergo flooring, with major features and interpreted causes being (A) very weak inflection at ~535 nm (Fe^{3+}), (B) weak inflection at 700 nm (Fe^{3+}), (C) 1200 nm (OH and C-H from cellulose), (D) 1430 nm (OH and H_2O), (E) 1720 nm (C-H), (F) 1900 nm (H_2O/OH cellulose), (G) 2100 (C-H, OH, and cellulose), and (H) 2310 nm (Mg-OH, Al-OH, and OH). Spectra for blush on dark brown carpet (Carpet 2) and blush on linoleum (Linoleum) are provided in the Supplementary Materials.
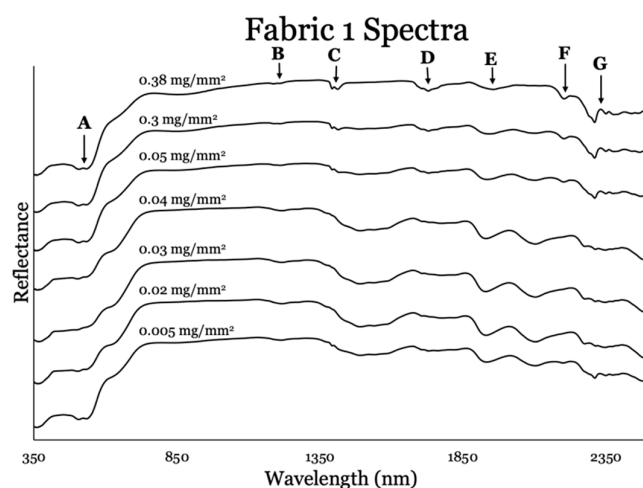
Figure 7. Spectra for clothing fabric. Spectra for blush on Fabric 1 (khaki), with major features and interpreted causes being (A) a doublet at 506 nm (S) and at ~535 nm (Fe^{3+}), (B) weak feature at 1205 nm (OH cotton), (C) 1392 nm and 1418 nm (OH and C-H), (D) 1730 nm (C-H), (E) 1932 nm (H_2O/OH cellulose), (F) 2200 nm (Al-OH, C-H, and C-O), and (G) 2310 nm (Mg-OH, Al-OH, and OH). Spectra for blush on Fabric 2 (denim) and Fabric 3 (white cotton) are provided in the Supplementary Materials.
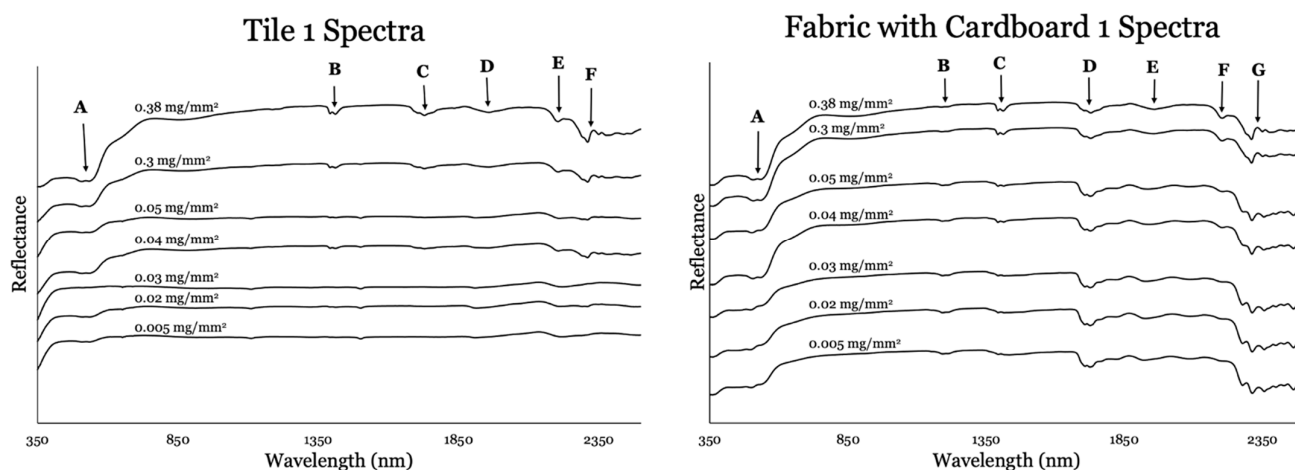
Figure 8. Materials related to bathrooms. Spectra for blush on white Tile 1, with some major features and interpreted causes being (A) weak doublet at ~506 nm (S) ~535 nm (Fe^{3+}), (B) doublet at 1397 nm and 1416 nm (H_2O and OH), (C) triplet with most intense at 1730 nm (C-H), (D) weak 1965 nm (C-OH), (E) 2200 nm (Al-OH, C-H, and C-O), and (F) 2310 nm (Mg-OH, Al-OH, and OH). Spectra for blush on light brown spectra for blush on khaki fabric with cardboard, with some major features and interpreted causes being (A) weak doublet at ~506 nm (S) ~535 nm (Fe^{3+}), (B) weak doublet at 1185 nm and 1205 nm (OH and C-OH), (C) 1205 nm (OH and C-H), (D) triplet (1710 nm, 1720 nm, and 1760 nm) grading to doublet at 1710 nm and 1720 nm (all (C-H)), (E) weak 1966 nm grading to 1947 nm (C-OH), (F) 2200 nm (Al-OH, C-H, and C-O), and (G) 2310 nm (Mg-OH, Al-OH, and OH). Spectra for blush on Tile 3 and on closet material are provided in the Supplementary Materials.

ASD analysis of Wet'N'Wild blush on these listed substrates demonstrated that makeup is detectable at the mg/mm² scale using remote sensing forensic techniques. This was established by comparing makeup-bearing substrates to the reference blush sample. Spectral analysis showed that Wet'N'Wild blush is detectable on substrates at an average of 0.03 mg/mm² (Table 1). The ASD spectra on certain substrates tend to show makeup on the ASD spectra at lower concentrations. This is attributed to these substrates being darker in color and therefore absorbing more light, while substrates which are lighter in color have a higher albedo and therefore will be more readily detected on the ASD.

In these scenarios, there is more interference within the spectra generated, and thus it is more challenging to discern the substrate from the makeup. For example, Carpet 2 is a dark brown color and has the lowest limit of detection at 0.02 mg/mm^2 (Table 1; Figure 6). There is less interference contributed by the darker substrates on the spectra due to the dark substrate absorbing light, making the makeup easier to detect at lower abundances. Substrates which are lighter in color, however, require higher concentrations of makeup in order for them to be detectable via spectral analysis. For example, Fabric 1 (khaki) and Fabric with Cardboard 1 (hanging organizer) had detection limits of 0.03 mg/mm^2 (Table 1; Figures 7 and 8), while other light-colored substrates, such as Wood Block 1, Tile 3, Pergo Wood 1, Linoleum 1, and Fabric 2, had detection limits of 0.05 mg/mm^2 (Table 1; Figures 6–9).
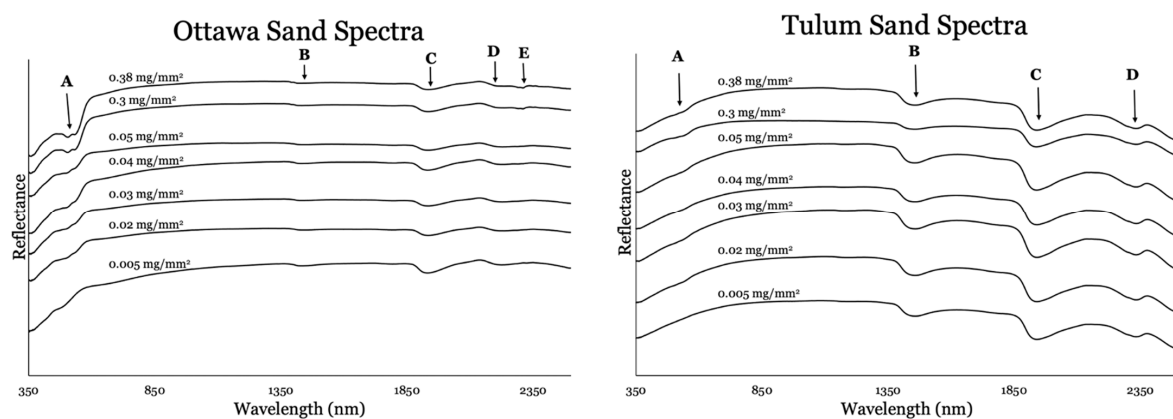
Figure 9. Outdoor materials. Spectra for blush on Ottawa sand, with major features and interpreted causes being (A) doublet at ~506 nm (S) and 535 nm (Fe^{3+}), (B) 1420 nm (OH), (C) 1940 nm (OH), (D) 2117 nm (OH), and (E) 2310 nm (Mg-OH, Al-OH, and OH). Spectra for blush on Tulum carbonate sand, with major features and interpreted causes being (A) weak inflection at ~535 nm (Fe^{3+}), (B) 1450 nm (H$_2$O), (C) 1900 nm (H$_2$O), and (D) 2350 nm (CO$_3^{2-}$). Blush is below the detection limit for the experimental conditions on Tulum carbonate sand. Spectra for blush on a pine wood block are provided in the Supplementary Materials.

Table 1. The smallest amount of makeup detected (limit of detection) on all substrates measured.

Substrate	Limit of Detection
Carpet 1	0.04 mg/mm^2
Carpet 2	0.02 mg/mm^2
Closet Material 1	0.03 mg/mm^2
Fabric 1	0.03 mg/mm^2
Fabric 1 with Cardboard	0.03 mg/mm^2
Fabric 2	0.05 mg/mm^2
Fabric 3	0.05 mg/mm^2
Linoleum 1	0.05 mg/mm^2
Ottawa Sand	0.03 mg/mm^2
Pergo Wood 1	0.05 mg/mm^2
Tile 1	0.03 mg/mm^2
Tile 3	0.05 mg/mm^2
Tulum Sand	>0.38 mg/mm^2
Wood Block 1	0.05 mg/mm^2

The minimum limit of detection across all makeup-bearing substrates was 0.02 mg/mm^2, with a maximum limit of detection of >0.38 mg/mm^2 (Table 2). The standard deviation amongst samples was 0.011 mg/mm^2 (excluding Tulum sand; Table 2). This establishes the variation in the limit of detection of blush between substrates that may be present in a crime scene. The mineralogical composition of the Wet'N'Wild blush samples was well characterized via powder XRD and is considered to be uniform at a level of a few wt. %. Thus, this further substantiates the interpretation of the limit of detection for this investigation.

Table 2. Maximum, minimum, average, and standard deviation values for limit of detection of measured substrates. Tulum sand is not accounted for in the average and standard deviation due to its detection limit being undetermined in this study.

Maximum	Minimum	Average	Standard Deviation
>0.38 mg/mm^2	0.02 mg/mm^2	0.03 mg/mm^2	0.01 mg/mm^2

4. Discussion

Reflective spectroscopy shows promise as a forensic investigative tool, as blush, used in this study as an analog material for mineral-based cosmetic products, can be detected in multiple and diverse substrates.

Powder XRD and TEM indicate that the cosmetic material investigated was mineralogically homogeneous and supports the minimal variation of the reflective spectra of the reference blush. The minerals observed by powder XRD are also consistent with the absorption and reflective features of the spectra collected.

Basic powder XRD is limited in use for the detailed investigation of phyllosilicates owing to the preferred orientation, overlapping peaks of some minerals, and sample preparation challenges [44,45]. Basic X-ray diffraction is, however, a method commonly used by forensic scientists despite these noted limitations. Numerous flaws exist with cosmetic industry methods, for example, the powder XRD portion of the CTFA J4-1 method intentionally induces orientation, uses preparation treatments that may remove or obscure analytical targets, and uses a limited range of scanning. Conservatively, basic powder XRD should be regarded as only being able to detect major phases within the context of phyllosilicate-dominated materials, which are present at several weight percent. These phases are the most likely to contribute to reflective spectra and dominate TEM observations. Thus, basic powder XRD is regarded as instructive during the study of these materials but not definitive.

Chlorite is commonly associated with talc (e.g., [46,47]); however, it should be noted that the (002) peak of chlorite (Figure 2) may have a contribution from serpentine, including chrysotile, which cannot be resolved using basic powder XRD. Serpentine minerals (e.g., lizardite, antigorite, and chrysotile) also have the potential to be associated with talc materials [47]. Additionally, it should be noted that there may be more than one chlorite composition present in this mixed-mineral material. Multiple chlorite and serpentine mixtures, if present, are not identifiable via the basic XRD methods. The observation of low-angle peaks may indicate that smectite minerals, or organo-smectite intercalates, and numerous organic ingredients are present in the blush. This is consistent with the ingredient list provided by the manufacturer (see Supplementary Table S1). These organic molecules have the potential to adsorb, exchange, or intercalate with any smectite or expandable mineral layers present. Accordingly, detailed investigations using more advanced clay mineral or phyllosilicate techniques are warranted for cosmetic materials in future studies in order to better define the nature of organo-mineral materials.

Asbestos content was not investigated in this study. Examples of talc particles were observed that conform to countable particles by the FDA's IWGACP December 2021 White Paper [48]. The concentration of these particles was not determined; however, these

findings merit further detailed TEM analysis using methods recommended by the IWGACP December 2021 White Paper.

To our knowledge, this is the first study to evaluate reflective spectra variation of a common (U.S.) brand of blush on numerous substrates that are representative of materials that have the potential to be encountered in crime scenes within the context of interpersonal violence. Variations in spectra were observed and were interpreted to be largely from diminished signal contributions correlative to diminishing mass. A range of detection limits was also observed. Data from this investigation have the potential to directly support hyperspectral imaging of indoor and outdoor crime scenes. Specifically, hyperspectral imaging is a remote sensing technique where images are acquired and, within an image, each pixel corresponds to a measured spectrum of a given wavelength, such as 350 nm to 2500 nm. Thus, hyperspectral imaging can also be used to detect and identify materials in a given scene, provided a library exists to identify such materials. Such approaches may be useful for documenting crime scenes before investigators enter and potentially disturb a space. In addition, the data reported in this work demonstrate the proof of concept and address potential variability. The blush used could hypothetically not have been detected on the numerous substrates evaluated, but limits of detection (average = 0.03 mg/mm^2) were clearly achieved. A next phase in this investigation could be to replicate the work under conditions of stress, including simulated water, high heat, and mechanical stressors.

Makeup-bearing substrates which were lighter were more variable, meaning that makeup was detected at varying concentrations. Closet material and Tile 1 both showed limits of detection of 0.03 mg/mm^2 (Table 1; Figure 8), while Fabric 3 (white cotton; Table 1, Figure 7) showed a limit of detection of 0.05 mg/mm^2. This is because the spectral characteristics of the substrates cause interference compared to the composition of the blush, which generates unique spectral features, making it more challenging to discern the makeup from the substrate.

The blush on sands, however, showed the most variety in the limit or nature of detection. The well-rounded, very quartz-rich, spectrally bright (white) Ottawa sand showed a limit of detection of 0.03 mg/mm^2 (Table 1; Figure 9), while the carbonate Tulum sand depicted the highest limit of detection among the substrates, as the limit was not determined and is therefore reported at >0.38 mg/mm^2 (Table 1; Figure 9). The comparatively high limit of detection of blush observed in the Tulum sand compared to the Ottawa sand (0.03 mg/mm^2) is likely related to the substrate's relatively high porosity and scatter, the shadow of grains, and the grain texture [49]. The Tulum sand is very porous owing to the presence of fossil materials, its high mechanical hardness, and the solubility variation of calcite and aragonite. High intragranular microporosity likely enables cosmetic material to be functionally sequestered or adsorbed within grains via intragranular porosity, resulting in a lower spectral yield. This is counterintuitive, as the Tulum sand is relatively spectrally bright (white) and would be expected to enable spectral distinction. However, this example documents the importance of understanding the physical characteristics of substrate materials.

The results of this investigation demonstrate the potential utility of using reflective spectroscopy, specifically the ASD spectroradiometer or similar instruments, with a blush product on a wide range of substrates and would support future studies which could assess a variety of different types of cosmetic materials. This study also opens the possibility of establishing a detailed reflective spectra and mineralogical database for makeup types on numerous substrates that can be used throughout the forensic sciences. Such a database could be integrated into existing databases [42] or hyperspectral imaging databases centered on human materials [42]. There is increasing interest in the use of hyperspectral imaging and technology for forensic purposes for materials relating to crime scenes and their investigation [50–52]. In the context of forensic study, hyperspectral imaging and technology has been demonstrated as useful, or to have potential use, for materials such as semen [53]; paper documents, including bank notes [51,54–56]; hidden graves and human remains [57]; as well as gunshot residue material [58,59] and stains involving blood [60,61].

The results of the present investigation on blush continue to support the development, integration, and application of hyperspectral imaging and technology.

Future investigations within these fields of study should incorporate a wide variety of cosmetic types and brands and include those that are representative and inclusive of varying skin tones and cultures. Although this study focused on one single type of cosmetic product purchased in the U.S. and demonstrated efficacy in detection, it is important to acknowledge that other types and styles of cosmetics exist and that multiple groups of people use similar cosmetics or specialty cosmetics. For example, cosmetics available for children and a range of entertainers or performers should also be studied.

The potential exists for crime scene investigators to use the portable ASD (PANalytical) FieldSpec 4 Hi-Res to identify the presence of makeup at a crime scene. With this context and knowledge, investigative efforts could then be made to link common materials or items to potential cosmetic products the victim(s) and the perpetrator(s) had access to and/or were known to wear. A comprehensive library would need to be systematically developed to support such forensic investigations, and specific methods would need to be developed to support effective prosecution.

Based on the findings presented, further research could yield a viable tool for gathering evidence in the assault of cosmetic wearers. Potential applications of such a tool include tracking the whereabouts of a victim, providing quantitative evidence in an investigation, and linking a victim to a potential suspect's property and/or vehicle (or mode of transportation) via the transfer of cosmetic material. Further investigation would include additional substrates as well as a wide range of makeup products (foundation, eyeshadow, lipstick, etc.) of varying brands. A more comprehensive spectral database would be useful to investigators and support the identification of more products via spectral analysis.

Critical to such uses would be the development of specific field protocols for collecting data with spectroradiometers, and such protocols may (and likely would) vary for indoor, outdoor, and physical conditions. Such protocols would ideally be developed in collaboration with forensic scientists, law enforcement officers, and prosecutors in order to establish the most effective and efficient approaches for all.

5. Conclusions

Reflective spectroscopy shows promise as a forensic investigative tool. Blush, used here as an analog for mineral-based cosmetics can be detected on multiple and diverse substrates. Through primary use of the ASD (PANalytical) FieldSpec 4 Hi-Res spectroradiometer, this study has documented that the Wet'N'Wild "Color Icon" blush in the shade "Pearlescent Pink" could be reliably detected on various indoor substrates. Specifically, small amounts of makeup, as low as 0.02 mg/mm^2, can be detected on common materials expected to be found in indoor environments (e.g., tile and carpet), as well as two representative sands as outdoor substrates. Average limits of detection (0.03 mg/mm^2) across substrates were achieved; however, the Tulum sand had a notably high limit of detection ($>0.38 \text{ mg/mm}^2$), indicating that further investigation is needed for substrates with more complex surface characteristics. The utility of the ASD spectroradiometer in these contexts has thus been demonstrated by this study, and future work should systematically focus on investigating a broad range of cosmetics (both type and manufacturer) used by a range of makeup wearers. Powder XRD data and TEM are broadly consistent and show minimal mineralogical variation. However, there appears to be a discrepancy between the XRD data collected and the ingredient list reported by the manufacturer for this particular cosmetic product. XRD and TEM data provide mineralogical constraints and aid in the interpretation of bond assignments. This study therefore demonstrates the feasibility of developing comprehensive spectral libraries which are optimized for the detection of cosmetic materials.

References

1. Moraes, J.D.D.; Bertolino, S.R.A.; Cuffini, S.L.; Ducart, D.F.; Bretzke, P.E.; Leonardi, G.R. Clay minerals: Properties and applications to dermocosmetic products and perspectives of natural raw materials for therapeutic purposes—A review. *Int. J. Pharm.* **2017**, *534*, 213–219. [CrossRef] [PubMed]
2. Kulikov, E.; Latham, K.; Adams, M.J. Classification and discrimination of some cosmetic face powders using XRF spectrometry with chemometric data analysis. *X-ray Spectrom.* **2012**, *41*, 410–415. [CrossRef]
3. O'Neill, E.; Harrington, D.; Allison, J. Interpretation of laser desorption mass spectra of unexpected inorganic species found in a cosmetic sample of forensic interest: Fingernail polish. *Anal. Bioanal. Chem.* **2009**, *394*, 2029–2038. [CrossRef] [PubMed]
4. Miranda-Bermudez, E.; Harp, B.P.; Barrows, J.N. Qualitative Identification of Permitted and Non-permitted Color Additives in Cosmetics. *J. AOAC Int.* **2014**, *97*, 1039–1047. [CrossRef]

5. Mercy, J.A.; Hillis, S.D.; Butchart, A.; Bellis, M.A.; Ward, C.L.; Fang, X.; Rosenberg, M.L. Chapter 5: Interpersonal Violence: Global Impact and Paths to Prevention. In *Injury Prevention and Environmental Health*, 3rd ed.; Mock, C.N., Nugent, R., Kobusingye, R., Smith, K.R., Eds.; The International Bank for Reconstruction and Development/The World Bank: Washington, DC, USA, 2017; Volume 7. [CrossRef]

6. Bergslein, E. *An Introduction to Forensic Geoscience*; Wiley-Blackwell: Hoboken, NJ, USA, 2012; 514p.

7. Chophi, R.; Sharma, S.; Sharma, S.; Singh, R. Trends in the forensic analysis of cosmetic evidence. *Forensic Chem.* **2019**, *14*, 100165. [CrossRef]

8. Gordon, A.; Coulson, S. The evidential value of cosmetic foundation smears in forensic casework. *J. Forensic Sci.* **2004**, *49*, 1244–1252. [CrossRef]

9. Adamowicz, M.S.; Labonte, R.D.; Schienman, J.E. The Potential of Cosmetic Applicators as a Sources of DNA for Forensic Analysis. *J. Forensic Sci.* **2015**, *4*, 1001–1011. [CrossRef]

10. López-López, M.; Vaz, J.; García-Ruiz, C. Confocal Raman spectrocopy for the analysis of nail polish evidence. *Talanta* **2014**, *138*, 155–162. [CrossRef]

11. Melquiades, F.L.; Parreira, P.S.; Endo, L.Y.; dos Santos, G.; Wouk, L.; Filho, O.P. Portable EDXRF for Quality Assurance of Cosmetics. *Cosmetics* **2015**, *2*, 277–285. [CrossRef]

12. Chophi, R.; Sharma, S.; Singh, R. Forensic analysis of red lipsticks using ATR-FTIR spectroscopy and chemometrics. *Forensic Chem.* **2020**, *17*, 100209. [CrossRef]

13. Kaur, K.; Yadav, P.K.; Bumbrah, G.S.; Sharma, R.M. Forensic classification of lipsticks using attenuated total reflectance—Fourier transform infrared (ATR-FTIR) spectroscopy. *Vib. Spectrosc.* **2020**, *110*, 103146. [CrossRef]

14. Chophi, R.; Sharma, S.; Singh, R. Discrimination of mail polish using attenuated total reflectance infrared reflectance spectroscopy and chemometrics. *Aust. J. Forensic Sci.* **2021**, *53*, 325–336. [CrossRef]

15. Gładysz, M.; Król, M.; Kościelniak, P. Current analytical methodologies used for examination of lipsticks and its traces for forensic purposes. *Microchem. J.* **2021**, *164*, 106002. [CrossRef]

16. Knijnenberg, A.; van Loon, A.; Dik, J.; van Asten, A. Elemental imaging of Forensic Traces with Macro and Micro-XRF. In *Leading Edge Techniques in Forensic Trace Evidence Analysis*; John Wiley: Hoboken, NJ, USA, 2022; pp. 213–244.

17. Khei, L.K.K.; Verma, R.; Tan, E.L.Y.; Ismail, D.; Asri, M.N.M. Forensic analysis of nail polish traces on different substrates using ATR-FTIR spectroscopy and chemometric methods. *Forensic Chem.* **2023**, *34*, 100503. [CrossRef]

18. Sacks, M.; Ackerman, A.R.; Shlosberg, A. Rape Myths in the Media: A Content Analysis of Local Newspaper Reporting in the United States. *Deviant Behav.* **2017**, *39*, 1237–1246. [CrossRef]

19. Pain, R. Space, sexual violence and social control: Integrating geographical and feminist analyses of women's fear of crime. *Prog. Hum. Geogr.* **1991**, *15*, 415–431. [CrossRef]

20. Krekeler, M.P.S.; Allen, C.S.; Kearns, L.E.; Maynard, J.B. An investigation of aspects of mine waste from a kyanite mine, Central Virginia, USA. *Environ. Earth Sci.* **2010**, *61*, 93–106. [CrossRef]

21. Cymes, B.A.; Almquist, C.B.; Krekeler, M.P.S. Europium-doped cryptomelane: Multi-pathway synthesis, characterization, and evaluation for the gas phase catalytic oxidation of ethanol. *Appl. Catal. A* **2020**, *589*, 117310. [CrossRef]

22. Cymes, I.; Szymczyk, S.; Sidoruk, M.; Cymes, I. Effect of River Supply on the Distribution of Macroelements in the Sediments of a Retention Reservoir—A Case Study of the Loje Reservoir. *Environ. Eng. Manag. J.* **2017**, *16*, 2869–2878. [CrossRef]

23. Paul, K.C.; Silverstein, J.; Krekeler, M.P.S. New insights into rare earth element particulate generated by cigarette lighters: An electron microscopy and materials science investigation of a poorly understood indoor air pollutant and constraints for urban geochemistry. *Environ. Earth Sci.* **2017**, *76*, 369. [CrossRef]

24. Burke, M.; Rakovan, J.; Krekeler, M.P.S. A study by electron microscopy of gold and associated minerals from Round Mountain, Nevada. *Ore Geol. Rev.* **2017**, *91*, 708–717. [CrossRef]

25. LeGalley, E.; Krekeler, M.P.S. A mineralogical and geochemical investigation of street sediment near a coal-fired power plant in Hamilton, Ohio: An example of complex pollution and cause for community health concerns. *Environ. Pollut.* **2013**, *176*, 26–35. [CrossRef]

26. Geaney, H.; Dickinson, C.; Barrett, C.A.; Ryan, K.M. High Density Germanium Nanowire Growth Directly from Copper Foil by Self-Induced Solid Seeding. *Chem. Mater.* **2011**, *23*, 4838–4843. [CrossRef]

27. Gatta, G.D.; Merlini, M.; Valdrè, G.; Liermann, H.-P.; Nénert, G.; Rothkirch, A.; Kahlenberg, V.; Pavese, A. On the crystal structure and compressional behavior of talc: A mineral of interest in petrology and material science. *Phys. Chem. Miner.* **2013**, *40*, 145–156. [CrossRef]

28. Bailey, S.W. X-ray Diffraction Identification of the Polytypes of Mica, Serpentine, and Chlorite. *Clays Clay Miner.* **1988**, *36*, 193–213. [CrossRef]

29. Allen, C.S.; Krekeler, M.P.S. Reflectance spectra of crude oils and refined petroleum products on a variety of common substrates. *SPIE* **2010**, *7687*, 162–174. [CrossRef]

30. Krekeler, M.P.S.; Allen, C.S. Remote sensing spectra of cesium chloride provide a potential emergency management tool for response to a radiological dispersal device detonation. *J. Emerg. Manag.* **2008**, *6*, 60–64. [CrossRef]

31. Oglesbee, T.; McLeod, C.L.; Chappell, C.; Vest, J.; Sturmer, D.; Krekeler, M.P.S. A mineralogical and geochemical investigation of modern aeolian sands near Tonopah, Nevada: Sources and environmental implications. *Catena* **2020**, *194*, 104640. [CrossRef]

32. Barnes, M.; McLeod, C.L.; Chappell, C.; Faraci, O.; Gibson, B.; Krekeler, M.P.S. Characterizing the geogenic background of the Midwest: A detailed mineralogical and geochemical investigation of a glacial till in southwestern Ohio. *Environ. Earth Sci.* **2020**, *79*, 159. [CrossRef]

33. Burke, M.; Dawson, C.; Allen, C.S.; Brum, J.; Roberts, J.; Krekeler, M.P.S. Reflective spectroscopy investigations of clothing items to support law enforcement, search and rescue, and war crime investigations. *Forensic Sci. Int.* **2019**, *304*, 109945. [CrossRef]

34. Wei, J.; Ming, Y.; Jia, Q.; Yang, D. Simple mineral mapping algorithm based on multitype spectral diagnostic absorption features: A case study at Cuprite, Nevada. *J. Appl. Remote Sens.* **2017**, *11*, 026015. [CrossRef]

35. Cloutis, E.A. Spectral Reflectance Properties of Hydrocarbons: Remote-Sensing Implications. *Science* **1989**, *245*, 165–168. [CrossRef] [PubMed]

36. Curran, P.J.; Dungan, J.L.; Gholz, H.L. Exploring the relationship between reflectance red edge and chlorophyll content in slash pine. *Tree Physiol.* **1990**, *7*, 33–48. [CrossRef]

37. Hunt, G.R. Spectral signatures of particulate minerals in the visible and near infrared. *Geophysics* **1977**, *42*, 501–513. [CrossRef]

38. Hunt, G.R.; Salisbury, J.; Lenhoff, C.J. Visible and near-infrared spectra of minerals and rocks III: Oxides and hydroxides. *Mod. Geol.* **1971**, *2*, 195–205.

39. Hunt, G.R.; Salisbury, J.W.; Lenhoff, C.J. Visible and near-infrared spectra of minerals and rocks IV: Sulphides and sulphates. *Mod. Geol.* **1971**, *3*, 1–14.

40. Hunt, G.R.; Logan, L.M. Variation of Single Particle Mid-Infrared Emission Spectrum with Particle Size. *Appl. Opt.* **1972**, *11*, 142–147. [CrossRef]

41. Hunt, G.R.; Salisbury, J.W.; Lenhoff, C.J. Visible and near-infrared spectra of minerals and rocks VI:additional silicates. *Mod. Geol.* **1973**, *4*, 85–106.

42. Krekeler, M.P.S.; Burke, M.; Allen, S.; Sather, B.; Chappell, C.; McLeod, C.L.; Loertscher, C.; Loertscher, S.; Dawson, C.; Brum, J.; et al. A novel hyperspectral remote sensing tool for detecting and analyzing human materials in the environment: A geoenvironmental approach to aid in emergency response. *Environ. Earth Sci.* **2023**, *82*, 109. [CrossRef]

43. Brum, J.; Schlegel, C.; Chappell, C.; Burke, M.; Krekeler, M.P.S. Reflective spectra of gasoline, diesel and jet fuel ion sand substrates under ambient and cold conditions: Implications for detection using hyperspectral remote sensing and development of age estimation models. *Environ. Earth Sci.* **2020**, *79*, 463. [CrossRef]

44. Bish, D.; Reynolds, R.C. Sample preparation for X-ray diffraction. In *Reviews in Mineralogy*; Bish, D.L., Post, J.E., Eds.; Mineralogical Society of America: Chantilly, VA, USA, 1989; Volume 20, pp. 73–99.

45. Moore, D.M.; Reynolds, R.C. *X-ray Diffraction and the Identification and Analysis of Clay Minerals*; Oxford University Press: New York, NY, USA, 1997.

46. Berg, R.B. *Talc and Chlorite Deposits in Montana*; Memoir 45; Montana Bureau of Mines and Geology Memoir: Butte, MT, USA, 1979; 3 sheets.

47. Evans, B.W.; Guggenheim, S. Talc, pyrophyllite, and related minerals. In *Reviews in Mineralogy*; Bailey, S.W., Ed.; Mineralogical Society of America: Chantilly, VA, USA, 1988; Volume 19, pp. 225–294.

48. Center for Food Safety and Applied Nutrition. White Paper: IWGACP Scientific Opinions on Testing Methods for Asbestos in Cosmetic Products Containing Talc. 2021. Available online: https://www.regulations.gov/document/FDA-2020-N-0025-0053 (accessed on 1 June 2023).

49. Krekeler, M.P.S.; Argyilan, E.P.; Lepp, J.; Kearns, L.E. Investigation of calcareous beach sands in the Akumal and Tulum areas for use in constructed wetlands, Eastern Yucatan Peninsula. *Environ. Earth Sci.* **2009**, *59*, 411–420. [CrossRef]

50. Edelman, G.J.; Aalders, M.C. Photogrammetry using visible, infrared, hyper-spectral and thermal imaging of crime scenes. *Forensic Sci. Int.* **2018**, *292*, 181–189. [CrossRef] [PubMed]

51. Khan, M.J.; Khan, H.S.; Yousaf, A.; Khurshid, K.; Abbas, A. Modern trends in hyperspectral image analysis: A review. *IEEE Access* **2018**, *6*, 14118–14129. [CrossRef]

52. Xu, J.Y.; Fang, S.B.; Zhou, J. Application of hyperspectral imaging and mass spectrometry imaging technique to fingerprinting visualization and trace analysis. *Acta Phys. Sin.* **2019**, *68*, 068701. [CrossRef]

53. Silva, C.S.; Pimentel, M.F.; Amigo, J.M.; Honorato, R.S.; Pasquini, C. Detecting semen stains on fabrics using near infrared hyperspectral images and multivariate models. *TrAC Trends Anal. Chem.* **2017**, *95*, 23–35. [CrossRef]

54. Brito, L.R.E.; Braz, A.; Honorato, R.S.; Pimentel, M.F.; Pasquini, C. Evaluating the potential of near infrared hyperspectral imaging associated with multivariate data analysis for examining crossing ink lines. *Forensic Sci. Int.* **2019**, *298*, 169–176. [CrossRef]

55. Qureshi, R.; Uzair, M.; Khurdid, K.; Yan, H. Hyperspectral document image processing: Applications, challenges and future prospects. *Pattern Recognit.* **2019**, *90*, 12–22. [CrossRef]

56. Lim, H.T.; Murukeshan, V.M. Hyperspectral imaging of polymer banknotes for building and analysis of spectral library. *Opt. Lasers Eng.* **2017**, *98*, 168–175. [CrossRef]

57. Murray, B.; Anderson, D.T.; Wescott, D.J.; Moorhead, R.; Anderson, M.F. Survey and Insights into unmanned aerial-vehicle-based detection and documentation of clandestine graves and human remains. *Hum. Biol.* **2018**, *90*, 45–61. [CrossRef]

58. Glomb, P.; Romaszewski, M.; Cholewa, M.; Domino, K. Application of hyper-spectral imaging and machine learning methods for the detection of gunshot residue patterns. *Forensic Sci. Int.* **2018**, *290*, 227–237. [CrossRef]

59. De Carvalho, M.A.; Talhavini, M.; Pimentel, M.F.; Amigo, J.M.; Pasquini, C.; Alves, S.; Weber, I.T. NIR hyperspectral images for identification of gunshot residue from tagged ammunition. *Anal. Methods* **2018**, *10*, 4711–4717. [CrossRef]

60. Cadd, S.; Li, B.; Beveridge, P.; O'Hare, W.T.; Islam, M. Age determination of blood stained fingerprints using visible wavelength reflectance hyperspectral imaging. *J. Imaging* **2018**, *4*, 141. [CrossRef]

61. Balash, A.; Holmes, K.; Burke, M.; Krekeler, M.P.S. Dirt, Blood, and Clothing: Reflective Spectroscopy investigations of human blood on geologic and other substrates to support forensic investigations. *Geol. Soc. Am. Abstr. Progr.* **2018**, *50*, 24. Available online: https://gsa.confex.com/gsa/2018AM/webprogram/Paper320767.html (accessed on 26 September 2023).